J|A|C|S ARTICLES

Published on Web 07/28/2010

New Light-Harvesting Molecular Systems Constructed with a Ru(II) Complex and a Linear-Shaped Re(I) Oligomer

Youhei Yamamoto,[†,‡,§] Yusuke Tamaki,[†] Tatsuto Yui,[†,‡] Kazuhide Koike,*[,||,‡] and Osamu Ishitani*[,†,‡]

Department of Chemistry, Graduate School of Science and Engineering, Tokyo Institute of Technology, 2-12-1-E1-9 O-okayama, Meguro-ku, Tokyo 152-8551, Japan, CREST, Japan Science and Technology Agency, and National Institute of Advanced Industrial Science and Technology (AIST), 16-1 Onogawa, Tsukuba, Ibaraki 305-8569, Japan

Received May 27, 2010; E-mail: ishitani@chem.titech.ac.jp

Abstract: A novel type of light-harvesting complexes was synthesized with a linear-shaped Re(I) oligomer as a photon absorber and a Ru(II) polypyridyl complex as an energy acceptor. The Re(I) oligomer and the Ru(II) complex are connected to each other with a bisdiimine ligand, that is, 1,2-bis[4-(4′-methyl-2,2′-bipyridinyl)]ethane (C2dmb). These Ru(II)−Re(I) multinuclear complexes, $[Ru(dmb)_2(C2dmb)Re(CO)_2\{-PP-Re(dmb)(CO)_2-PP-Re(dmb)(CO)_3\}_2](PF_6)_7$, $[Ru(dmb)_2(C2dmb)Re(CO)_2\{-PP-Re(dmb)(CO)_3\}_2](PF_6)_5$, and $[Ru(dmb)_2(C2dmb)Re(CO)_3-PP-Re(dmb)(CO)_2-PP-Re(dmb)(CO)_3](PF_6)_5$ (dmb = 4,4′-dimethyl-2,2′-bipyridine; PP = bis(diphenylphosphino)acetylene), can strongly absorb a wide range of UV−vis light and emit mostly from the ^{3}MLCT excited state of the Ru(II) unit at room temperature in solution even when the Re chain absorbs the light. Comparison of their photophysical properties with those of the corresponding model complexes shows that a highly efficient energy transfer from the Re chain to the Ru(II) unit occurs, and the energy transfer rate constants from each Re(I) unit were determined.

Introduction

Photon collection is one of the most important functions in solar energy harvesting devices such as solar batteries[1−3] and photocatalysts for CO_2 reduction and hydrogen evolution.[4−12] When photosynthesis occurs in nature, well-ordered assemblies that contain many chlorophylls collect the solar light and transfer it to the reaction center.[13−15] Some artificial molecular-based photon-collection systems have been reported. Polypyridyl complexes of d^6 transition metal ions such as ruthenium(II),[16] osmium(III),[17] iridium(III),[18] and rhenium(I)[19] are the light absorbers that are used most often because of their outstanding photophysical properties, which include the long lifetime of the triplet metal-to-ligand charge transfer (^{3}MLCT) excited state and the high emission quantum yield at ambient temperature even in solution. Polymers that include these metal complexes have been synthesized for use in light collection systems. However,

[†] Tokyo Institute of Technology.
[‡] CREST/JST.
[§] Present address: Department of Pharmacy, College of Pharmaceutical Sciences, Ritsumeikan University, 1-1-1 Nojihigasi, Kusatsu, Shiga 525-8577, Japan.
[||] AIST.

(1) Nocera, D. G. *Inorg. Chem.* **2009**, *48*, 10001–10017.
(2) Zakeeruddin, S. M.; Grätzel, M. *Adv. Funct. Mater.* **2009**, *19*, 2187–2202.
(3) Zhang, Z.; Zakeeruddin, S. M.; O'Regan, B. C.; Humphry-Baker, R.; Grätzel, M. *J. Phys. Chem. B* **2005**, *109*, 21818–21824.
(4) Morris, A. J.; Meyer, G. J.; Fujita, E. *Acc. Chem. Res.* **2009**, *42*, 1983–1994.
(5) Hung, C.-Y.; Singh, A. S.; Chen, C.-W.; Wen, Y.-S.; Sun, S.-S. *Chem. Commun.* **2009**, 1511–1513.
(6) Kanan, M. W.; Surendranath, Y.; Nocera, D. G. *Chem. Soc. Rev.* **2009**, *38*, 109–114.
(7) Takeda, H.; Koike, K.; Inoue, H.; Ishitani, O. *J. Am. Chem. Soc.* **2008**, *130*, 2023–2031.
(8) Esswein, A. J.; Nocera, D. G. *Chem. Rev.* **2007**, *107*, 4022–4047.
(9) Arakawa, H.; et al. *Chem. Rev.* **2001**, *101*, 953–996.
(10) Fujita, E.; DuBois, D. L. *Carbon Dioxide Fixation*; BNL-67078, Brookhaven National Laboratory: Upton, NY, 2000; pp 1−34.
(11) Heyduk, A. F.; Nocera, D. G. *Science* **2001**, *293*, 1639–1641.
(12) Amouyal, E. In *Homogeneous Photocatalysis*; Chanon, M., Ed.; VCH: Weinheim, Germany, 1997; Vol. 2, pp 263−307.
(13) Scheer, H. In *Light Harvesting Antennas in Photosynthesis*; Green, B. R., Parson, W. W., Eds.; Kluwer Academic: Dordrecht, 2003; Vol. 29, p 81.
(14) Tamiaki, H.; Shibata, R.; Mizoguchi, T. *Photochem. Photobiol.* **2007**, *83*, 152–162.
(15) Mizoguchi, T.; Nagai, C.; Kunieda, M.; Kimura, Y.; Okamura, A.; Tamiaki, H. *Org. Biomol. Chem.* **2009**, *7*, 2120–2126.
(16) (a) Harriman, A.; Khatyr, A.; Ziessel, R. *Res. Chem. Intermed.* **2007**, *33*, 49–62. (b) Campagna, S.; Serroni, S.; Bodige, S.; MacDonnell, F. M. *Inorg. Chem.* **1999**, *38*, 692–701. (c) Balzani, V.; Campagna, S.; Denti, G.; Juris, A.; Serroni, S.; Venturi, M. *Acc. Chem. Res.* **1998**, *31*, 26–34.
(17) (a) Wu, P. C.; Yu, J. K.; Song, Y. H.; Chi, Y.; Chou, P. T.; Peng, S. M.; Lee, G. H. *Organometallics* **2003**, *22*, 4938–4946. (b) Argazzi, R.; Bertolasi, E.; Chiorboli, C.; Bignozzi, C. A.; Itokazu, M. K.; Murakami Iha, N. Y. *Inorg. Chem.* **2001**, *40*, 6885–6891. (c) Furue, M.; Yoshidzumi, T.; Kinoshita, S.; Kushida, T.; Nozakura, S.; Kamachi, M. *Bull. Chem. Soc. Jpn.* **1991**, *64*, 1632–1640.
(18) (a) Neve, F.; Crispini, A.; Serroni, S.; Loiseau, F.; Campagna, S. *Inorg. Chem.* **2001**, *40*, 1093–1101. (b) Bolink, H. J.; Coronado, E.; Santamaria, S. G.; Sessolo, M.; Evans, N.; Klein, C.; Baranoff, E.; Kalyanasundaram, K.; Grätzel, M.; Nazeeruddin, M. K. *Chem. Commun.* **2007**, 3276–3278. (c) Wong, W.-Y.; Ho, C. -L. *Coord. Chem. Rev.* **2009**, *253*, 1709–1758.
(19) (a) Wolcan, E.; Féliz, M. R. *Photochem. Photobiol. Sci.* **2003**, *2*, 412–417. (b) Xue, W.-M.; Goswami, N.; Eichhorn, D. M.; Orizonde, P. L.; Rillema, D. P. *Inorg. Chem.* **2000**, *39*, 4460–4467. (c) Bardwell, D. A.; Barigelletti, F.; Cleary, R. L.; Flamigni, L.; Guardigli, M.; Jeffery, J. C.; Ward, M. D. *Inorg. Chem.* **1995**, *34*, 2438–2446. (d) Sullivan, B. P. *J. Phys. Chem.* **1989**, *93*, 24–26.

the metal complexes often hang from an organic polymer chain as pendant groups[20,21] or π-conjugated heteroaromatic polymers with diimine parts in a main chain coordinated with metal complexes.[22−24] On the other hand, only a few emissive polymers have been reported with main chains that are held together by transition-metal complexes.[25−32] These complexes should have unique properties because of the contribution of the d-orbitals in the transition metal ions to the main polymer chain.

We recently reported the systematic synthesis of linear-shaped Re(I) multinuclear complexes bridged with bidentate phosphorus ligands that have 2−20 Re(I) units in the backbone of the polymer chain (Scheme 1).[33] These complexes can strongly emit at ambient temperature even in solution. Furthermore, in these oligomers and polymers, the photochemical energy transfer occurs efficiently from the edge unit to the interior units.

Here, we report a new series of light-harvesting systems with the linear-shaped Re(I) oligomer as a photon absorber and a Ru(II) polypyridyl complex as an energy acceptor. The Re(I) oligomer and Ru(II) complex are connected to each other by a bisdiimine ligand (Scheme 2).

Results and Discussion

Synthesis. Scheme 2 summarizes the synthesis procedure for the Ru(II)−Re(I) multinuclear complexes. The Ru(II)−Re(I) dinuclear complex, $[Ru(dmb)_2(C2dmb)Re(CO)_3(CF_3SO_3)]^{2+}$ (dmb = 4,4′-dimethyl-2,2′-bipyridine, C2dmb = 1,2-bis[4-(4′-methyl-2,2′-bipyridinyl)]ethane) (**Ru−Re(CO)$_3$(CF$_3$SO$_3$)**$^{2+}$), can be quantitatively obtained by the reaction of $[Ru(dmb)_2(C2dmb)Re(CO)_3Cl]^{2+}$ (**Ru−Re(CO)$_3$Cl**$^{2+}$) with an equal amount of $Tl(CF_3SO_3)$ in CH_2Cl_2[34] followed by excess bis(diphenylphosphino)acetylene (**PP**) in CH_2Cl_2. The result is $[Ru(dmb)_2(C2dmb)Re(CO)_3(\eta^1\text{-PP})]^{3+}$ (**Ru−Re(CO)$_3$(η^1-PP)**$^{3+}$), where **PP** works as a monodentate ligand and can potentially coordinate with another metal center.

Scheme 1. Structures and Abbreviations of the Linear-Shaped Re(I) Multinuclear Complexes and the Ru(II)−Re(I) Dinuclear Complex as Model Compounds

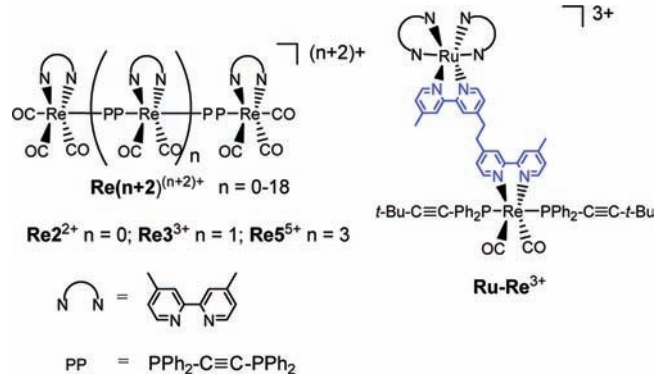

Photochemical ligand substitution of the Re(I) unit in this binuclear complex is one of the key steps for synthesis of **Ru−Re3A**$^{3+}$ and **Ru−Re5**$^{7+}$. Irradiation of a THF−CH_2Cl_2 mixed solution containing **Ru−Re(CO)$_3$(η^1-PP)**$^{3+}$ and excess **PP** at 50−60 °C gave $[Ru(dmb)_2(C2dmb)Re(CO)_2(\eta^1\text{-PP})_2]^{3+}$ (**Ru−Re(CO)$_2$(η^1-PP)$_2$**$^{3+}$). We have reported the photochemical ligand substitution reaction of the Re(I) mononuclear complexes with a phosphorus ligand, where only the CO ligand in the trans position to the phosphorus ligand is substituted via a thermal transition from the lowest excited state (i.e., ^{3}MLCT) to the ligand field (LF) excited state.[35,36] In the case of the Ru(II)−Re(I) binuclear complex, however, the ligand substitution of the Re(I) unit competed with the energy transfer from the ^{3}MLCT excited state of the Re(I) unit to the Ru(II) unit. Irradiation at a higher temperature made the photochemical ligand substitution more favorable than the energy transfer.

A dichloromethane solution containing **Ru−Re(CO)$_2$(η^1-PP)$_2$**$^{3+}$ and 2 equiv of *fac*-$Re(dmb)(CO)_3(CF_3SO_3)$ was stirred at room temperature for 1 day and then heated at 40 °C for 1 more day. The result was **Ru−Re3A**$^{3+}$ in a 16% isolated yield based on the starting dinuclear complex **Ru−Re(CO)$_3$Cl**$^{2+}$ used. A similar method was successfully applied to synthesize **Ru−Re5**$^{7+}$ using the Re(I) dimer $[Re(dmb)(CO)_3\text{−}PP\text{−}Re(dmb)(CO)_2(CF_3SO_3)]^+$, which has an easily replaceable $CF_3SO_3^-$ anion coordinated in the trans position to a phosphorus bridge ligand, instead of *fac*-$Re(dmb)(CO)_3(CF_3SO_3)$. The isolated yield was 13%. Another tetranuclear complex, **Ru−Re3B**$^{5+}$, has the Ru(II) unit attached to one of the

(20) (a) Friesen, D. A.; Kajita, T.; Danielson, E.; Meyer, T. J. *Inorg. Chem.* **1998**, *37*, 2756–2762. (b) Dupray, L. M.; Devenney, M.; Striplin, D. R.; Meyer, T. J. *J. Am. Chem. Soc.* **1997**, *119*, 10243–10244. (c) Jones, W. E.; Baxter, S. M.; Strouse, G. F.; Meyer, T. J. *J. Am. Chem. Soc.* **1993**, *115*, 1363–7373.
(21) Serin, J.; Schultze, X.; Adronov, A.; Frechet, J. M. J. *Macromolecules* **2002**, *35*, 5396–5404.
(22) (a) Harriman, A.; Khatry, A.; Ziessel, R. *Res. Chem. Intermed.* **2007**, *33*, 49–62. (b) Harriman, A.; Rostron, S. A.; Khatyr, A.; Ziessel, R. *Faraday Discuss.* **2006**, *131*, 377–391. (c) Harriman, A.; Ziessel, R. *Coord. Chem. Rev.* **1998**, *171*, 331–339. (d) Goeb, S.; DeNicola, A.; Ziessel, R. *J. Organomet. Chem.* **2005**, *70*, 6802–6808.
(23) Connors, P. J.; Tzalis, D.; Dunnick, A. L.; Tor, Y. *Inorg. Chem.* **1998**, *37*, 1121–1123.
(24) (a) Hayasida, N.; Yamamoto, T. *Bull. Chem. Soc. Jpn.* **1999**, *72*, 1153–1162. (b) Yamamoto, T.; Maruyama, T.; Zhou, Z.-H.; Ito, T.; Fukuda, T.; Yoneda, Y.; Begum, F.; Ikeda, T.; Sasaki, S.; Takezoe, H.; Fukuda, A.; Kubotall, K. *J. Am. Chem. Soc.* **1994**, *116*, 4832–4845.
(25) Hissler, M.; El-ghayoury, A.; Harriman, A.; Ziessel, R. *Angew. Chem., Int. Ed.* **1998**, *37*, 1717–1720.
(26) Knapp, R.; Kelch, S.; Schmelz, O.; Rehahn, M. *Macromol. Symp.* **2003**, *204*, 267–286.
(27) Cho, T. J.; Moorefield, C. N.; Hwang, S.-H.; Wang, P.; Godínez, L. A.; Bustos, E.; Newkome, G. R. *Eur. J. Org. Chem.* **2006**, 4193–4200.
(28) (a) Yam, V. W. W.; Wong, K. M. C. In *Molecular Wires*; De Cola, L., Ed.; Springer: Berlin, 2005; Vol. 257, pp 1−32. (b) Yam, V. W. W.; Cheng, E. C. C. In *Photochemistry and Photophysics of Coordination Compounds II*; Balzani, V., Campagna, S., Eds.; Springer: Berlin, 2007; Vol. 281, pp 269−310. (c) Yam, V. W. W.; Lo, K. K. W.; Wong, K. M. C. *J. Organomet. Chem.* **1999**, *578*, 3–30.
(29) Vicente, J.; Chicote, M. T.; Alvarez-Falcon, M. M.; Fox, M. A.; Bautista, D. *Organometallics* **2003**, *22*, 4792–4797.
(30) (a) Yamamoto, Y.; Shiotsuka, M.; Onaka, S. *J. Organomet. Chem.* **2004**, *689*, 2905–2911. (b) Shiotsuka, M.; Yamamoto, Y.; Okuno, S.; Kitou, M.; Nozaki, K.; Onaka, S. *Chem. Commun.* **2002**, 590–591.
(31) (a) Hissler, M.; El-ghayoury, A.; Harriman, A.; Ziessel, R. *Angew. Chem., Int. Ed.* **1998**, *37*, 1717–1720. (b) Harriman, A.; Ziessel, R. *Coord. Chem. Rev.* **1998**, *171*, 331–339. (c) Benniston, A. C.; Harriman, A.; Li, P.; Patel, P. V.; Sams, C. A. *Chem.-Eur. J.* **2008**, *14*, 1710–1717. (d) Barigelletti, F.; Flamigni, L.; Balzani, V.; Collin, J.-P.; Sauvage, J.-P.; Sour, A.; Constable, E. C.; Thompson, A. M. W. C. *J. Am. Chem. Soc.* **1994**, *116*, 7692–7699.
(32) (a) Wong, W.-Y.; Harvey, P. D. *Macromol. Rapid Commun.* **2010**, *31*, 671–713. (b) Wong, W.-Y. *Macromol. Chem. Phys.* **2008**, *209*, 14–24.
(33) (a) Yamamoto, Y.; Sawa, S.; Funada, Y.; Morimoto, T.; Falkenström, M.; Miyasaka, H.; Shishido, S.; Ozeki, T.; Koike, K.; Ishitani, O. *J. Am. Chem. Soc.* **2008**, *130*, 14659–14674. (b) Ishitani, O.; Kanai, K.; Yamada, Y.; Sakamoto, K. *Chem. Commun.* **2001**, 1514–1515.
(34) Sato, S.; Koike, K.; Inoue, H.; Ishitani, O. *Photochem. Photobiol. Sci.* **2007**, *6*, 454–461.
(35) Koike, K.; Tanabe, J.; Toyama, S.; Tsubaki, H.; Sakamoto, K.; Westwell, J. R.; Johnson, F. P. A.; Hori, H.; Saitoh, H.; Ishitani, O. *Inorg. Chem.* **2000**, *39*, 2777–2783.
(36) Koike, K.; Okoshi, N.; Hori, H.; Takeuchi, K.; Ishitani, O.; Tsubaki, H.; Clark, I. P.; George, M. W.; Johnson, F. P. A.; Turner, J. J. *J. Am. Chem. Soc.* **2002**, *124*, 11448–11455.

Scheme 2. Synthesis of the Ru(II)−Re(I) Multinuclear Complexes[a]

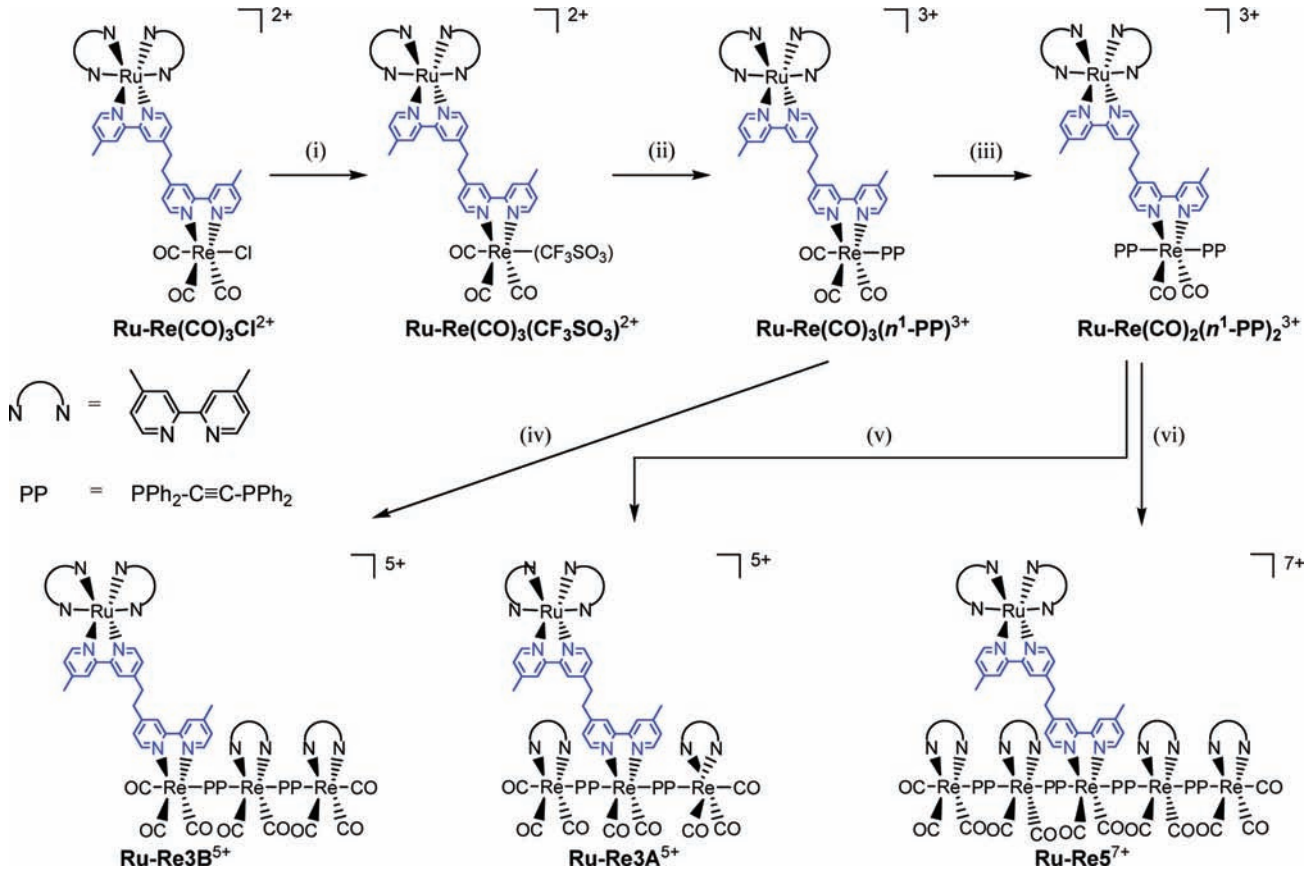

[a] Reagents and reaction conditions: (i) $Tl(CF_3SO_3)$ (1 equiv) in CH_2Cl_2 reflux for 2 days; (ii) an excess **PP** in CH_2Cl_2 at room temperature for 1 day and then at 40 °C for 1 day; (iii) *hν* (>330 nm) in CH_2Cl_2/THF (1:1) containing an excess **PP** at 50−60 °C for 8 h; (iv) $[Re(dmb)(CO)_3-\mathbf{PP}-Re(dmb)(CO)_2(CF_3SO_3)]^+$ (1 equiv) in CH_2Cl_2 at room temperature for 1 day and then at 40 °C for 1 day; (v) *fac*-$Re(dmb)(CO)_3(CF_3SO_3)$ (2 equiv) in CH_2Cl_2 at room temperature for 1 day and then at 40 °C for 1 day; and (vi) $[Re(dmb)(CO)_3-\mathbf{PP}-Re(dmb)(CO)_2(CF_3SO_3)]^+$ (2 equiv) in CH_2Cl_2 at room temperature for 1 day and then at 40 °C for 1 day.

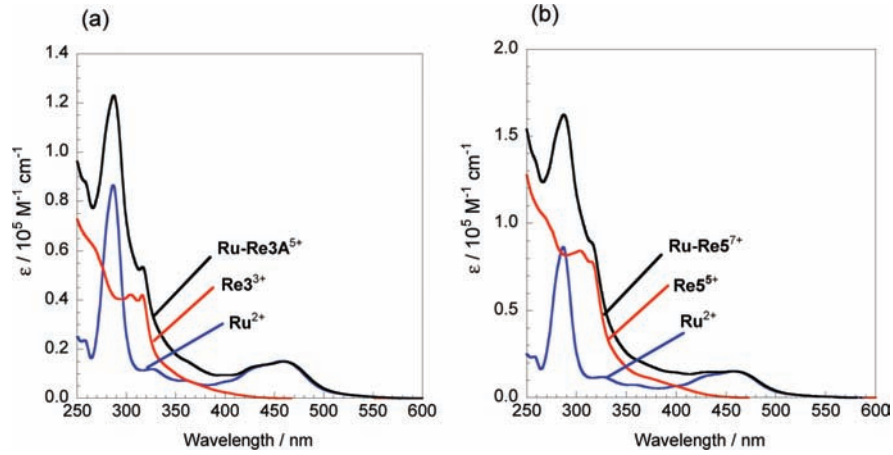

Figure 1. UV/vis absorption spectra of MeCN solutions containing (a) **Ru**−**Re3A**$^{5+}$ (black line), **Re3**$^{3+}$ (red line), and **Ru**$^{2+}$ (blue line); and (b) **Ru**−**Re5**$^{7+}$ (black line), **Re5**$^{5+}$ (red line), and **Ru**$^{2+}$ (blue line).

edges of the trinuclear Re(I) unit. This complex was obtained by the reaction of the **Ru**−**Re(CO)$_3$(η^1-PP)**$^{3+}$ with $[Re(dmb)(CO)_3-\mathbf{PP}-Re(dmb)(CO)_2(CF_3SO_3)]^+$. The isolated yield was 21%. All of the Ru(II)−Re(I) multinuclear complexes were isolated by size exclusion chromatography (SEC)[37] and identified by ^{1}H NMR, IR, electrospray ionization mass spectrometry, analytical SEC, and elemental analysis (see the Supporting Information).

Photophysical Properties. As a typical example, Figure 1a shows the UV/vis absorption spectra of **Ru**−**Re3A**$^{5+}$ and the corresponding model complexes, that is, the Ru(II) mononuclear complex $[Ru(dmb)_3]^{2+}$ (**Ru**$^{2+}$) and the Re(I) trimer $[Re(dmb)(CO)_3-\mathbf{PP}-Re(dmb)(CO)_2-\mathbf{PP}-Re(dmb)(CO)_3]^{3+}$

(37) Takeda, H.; Yamamoto, Y.; Nishiura, C.; Ishitani, O. *Anal. Sci.* **2006**, *22*, 545–549.

Table 1. Absorption Maxima and Molar Extinction Coefficients of Ru(II)−Re(I) Multinuclear Complexes and the Corresponding Model Complexes[a]

complex	λ_{abs} nm ($\varepsilon/10^4$ M^{-1} cm^{-1})				
Ru−**Re3A**$^{5+}$	286 (12.1)	314 (5.1)	350 (1.8)	390 (1.1)	460 (1.5)
Ru−**Re3B**$^{5+}$	285 (13.8)	315 (5.7)	350 (1.8)	390 (1.1)	460 (1.5)
Ru−**Re5**$^{7+}$	285 (16.1)	314 (8.9)	350 (2.6)	390 (1.5)	460 (1.5)
Re2^{2+}		315 (2.6)	350 (0.7)		
Re3^{3+}		315 (4.1)	350 (1.0)	390 (0.3)	
Re5^{5+}		314 (7.8)	350 (1.8)	390 (0.7)	
Ru^{2+}	286 (8.6)				460 (1.5)

[a] Measured in an MeCN solution at 25 °C.

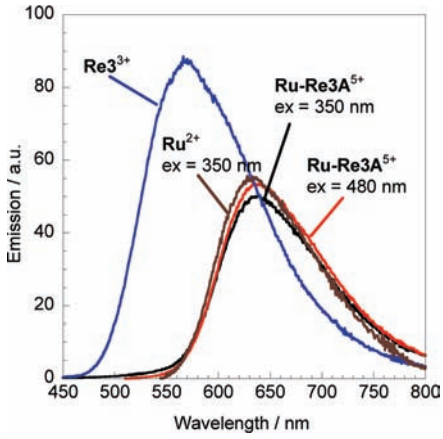

Figure 2. Emission spectra of degassed MeCN solutions containing **Ru**−**Re3A**$^{5+}$ by excitation at 350 nm (black line) and 480 nm (red line), **Re3**$^{3+}$ by excitation at 350 nm (blue line), and **Ru**$^{2+}$ by excitation at 350 nm (brown line). They are standardized by the number of absorbed photons at the excitation wavelength.

(**Re3**$^{3+}$). The spectrum of **Ru**−**Re3A**$^{5+}$ was almost identical to the 1:1 summation spectrum of **Ru**$^{2+}$ and **Re3**$^{3+}$. This result indicates that no strong electronic interaction occurred in the ground state between the Ru(II) and Re(I) units, and the absorptions at 330−400 and 410−490 nm of **Ru**−**Re3A**$^{5+}$ can be assigned to the ^{1}MLCT absorption bands of the Re chain and the Ru(II) unit, respectively. The strong absorption around 290 nm is attributed to the $\pi-\pi^*$ absorption bands of the diimine ligands on both the Re(I) and the Ru(II) units. Similar results were obtained for both **Ru**−**Re3B**$^{5+}$ and **Ru**−**Re5**$^{7+}$ (Figure S4). Table 1 summarizes the UV/vis absorption properties of the Ru(II)−Re(I) multinuclear complexes and the corresponding model complexes. It is noteworthy that these multinuclear complexes strongly absorb a very wide range of UV and visible light. For example, **Ru**−**Re5**$^{7+}$ absorbs light with $\varepsilon > 10^4$ M^{-1} cm^{-1} at all UV−vis wavelengths shorter than 480 nm (Figure 1b).

All of the Ru(II)−Re(I) multinuclear complexes emit, mostly from the Ru(II) unit, at room temperature in solution even when the Re chain absorbs light. Figure 2 shows the emission spectra of **Ru**−**Re3A**$^{5+}$ using 350 nm light for excitation. The emission spectra of both **Re3**$^{3+}$ upon excitation at 350 nm and **Ru**−**Re3A**$^{5+}$ at 480 nm (the light is only absorbed by the Ru(II) unit in the complex) are also illustrated in Figure 2. The emission spectrum of **Re3**$^{3+}$, which is the model compound for the Re chain in **Ru**−**Re3A**$^{5+}$, had a broad band with an emission maximum at 560 nm ($\Phi = 0.16$). On the other hand, emission of **Ru**−**Re3A**$^{5+}$ had a maximum at 638 nm using the same excitation light that was absorbed by both the Re(I) units and the Ru(II) unit with a 5.7:4.3 ratio, which was calculated using both molecular extinction coefficients of the models **Re3**$^{3+}$ ($\varepsilon_{350\ nm} = 10.0 \times 10^3$ M^{-1} cm^{-1}) and **Ru**$^{2+}$ ($\varepsilon_{350\ nm} = 7.4 \times 10^3$ M^{-1} cm^{-1}). This emission spectrum was similar to both the spectrum of **Ru**−**Re3A**$^{5+}$ that was excited using 480 nm light, which is absorbed by only the Ru(II) unit, and the spectrum of the model of Ru(II) unit (**Ru**$^{2+}$).

These results clearly indicate that the emission occurs mainly from the Ru(II) unit in **Ru**−**Re3A**$^{5+}$ even when the Re chain is excited because efficient intramolecular energy transfer occurs from the excited Re chain to the Ru(II) unit. If the shapes and efficiencies of both emission from the Re chain and the Ru(II) unit of **Ru**−**Re3A**$^{5+}$ are the same as those of **Re3**$^{3+}$ and **Ru**$^{2+}$, then the emission spectrum of **Ru**−**Re3A**$^{5+}$ ($I_{Ru-Re3A^{5+}}$) that is excited using 350 nm light can be simulated by the linear sum of spectra of **Re3**$^{3+}$ and **Ru**−**Re3A**$^{5+}$ that is excited using 480 nm light ($I_{Re^{3+}}$ and $I_{Ru^{2+}}$) as shown in the following equation:[38]

$$I_{Ru-Re3A^{5+}} = \frac{\varepsilon_{Re^{3+}}}{\varepsilon_{Ru\text{-}Re3A^{5+}}} \times I_{Re^{3+}} \times \alpha + \frac{\varepsilon_{Ru^{2+}}}{\varepsilon_{Ru-Re3A^{5+}}} \times I_{Ru^{2+}} \times \beta \quad (1)$$

where $\varepsilon_{Ru-Re3A^{5+}}$, $\varepsilon_{Re^{2+}}$, and $\varepsilon_{Ru^{3+}}$ are the molar extinction coefficients of **Ru**−**Re3A**$^{5+}$, **Ru**$^{2+}$, and **Re3**$^{3+}$ at 350 nm, and α and β are the ratios of the emission intensities from the Re chain and the Ru(II) unit in **Ru**−**Re3A**$^{5+}$ to those of **Re3**$^{3+}$ and the Ru(II) unit when the photons absorbed by them are equal to those absorbed by the Ru(II) unit and the Re chain in **Ru**−**Re3A**$^{5+}$, respectively. The nonlinear least-squares method was applied for fitting the spectral data shown in Figure 2, giving $\alpha = 0.033$ and $\beta = 2.134$ as the best-fitted data. These data strongly indicate that the energy transfer occurred from the excited Re chain to the Ru(II) unit with an efficiency of 86%.

Similar measurements and analyses were applied to **Ru**−**Re3B**$^{5+}$ and **Ru**−**Re5**$^{7+}$. In both cases, efficient energy transfer from the excited Re chain to the Ru(II) unit was observed, and energy transfer efficiencies of 85% and 77% were obtained for **Ru**−**Re3B**$^{5+}$ and **Ru**−**Re5**$^{7+}$, respectively (Figure S5).

Using the single-photon-counting technique, the emission lifetimes of the Ru−Re multinuclear complexes and their models were measured using 350 nm excitation light. The emission decay of **Ru**−**Re3A**$^{5+}$ could be fitted with triple-exponential functions with lifetimes of 8, 133, and 902 ns (Figure 3) as follows:[39]

$$I(t) = A_1 e^{-t/\tau_1} + A_2 e^{-t/\tau_2} + A_3 e^{-t/\tau_3} \quad (2)$$

where $I(t)$, A_n, and τ_n are intensities of the emission at time t, pre-exponential factors, and lifetimes, respectively. The propor-

(38) The emission spectra from the Ru(II) units in **Ru**−**Re3A**$^{5+}$, **Ru**−**Re3B**$^{5+}$, and **Ru**−**Re5**$^{7+}$ were slightly different from that from **Ru**$^{2+}$ ($\Delta\lambda_{max} = 3$ nm) because of very week interaction between the Ru(II) unit and the Re(I) unit attached to the Ru(II) unit through the bridge ligand: Koike, K.; Naito, S.; Sato, S.; Tamaki, Y.; Ishitani, O. *J. Photochem. Photobiol., A* **2009**, *207*, 109. The emission spectra from the Re chain in the Ru−Re systems might be also slightly different from the corresponding Re oligomers because of the same interaction; even so, we have to use the emission spectra from the corresponding Re oligomers because emission only from the Re chain in the Ru−Re systems cannot be obtained due to the energy transfer. However, an error caused by this should not conspicuously affect the estimation of the energy transfer efficiency because the fitting data were much more strongly dependent on the emission from the Ru(II) unit than that from the Re chain.

(39) Although the time resolution of the emission decay measurements was sub nanosecond, no faster decay was detected than those shown in Figure 3.

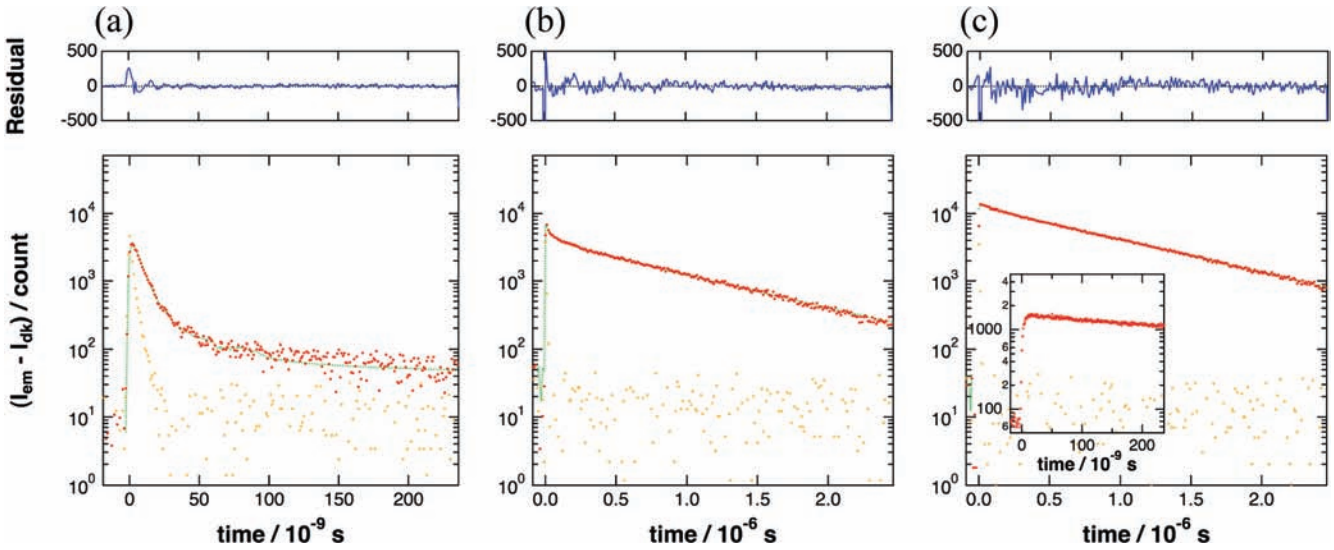

Figure 3. Emission decay curves of **Ru**−**Re3A**$^{5+}$ obtained at an excitation wavelength of 350 nm. Monitor wavelengths were 470 nm (a), 570 nm (b), and 620 nm (c).

Table 2. Photophysical Properties of Ru(II)−Re(I) Multinuclear Complexes and the Corresponding Re(I) Oligomers[a]

			lifetime/ns			pre-exponential factors[d]/%								
						observed at 480 nm			observed at 570 nm			observed at 620 nm		
complex	λ_{em}[b]	Φ_{em}[c]	τ_1	τ_2	τ_3	a_1	a_2	a_3	a_1	a_2	a_3	a_1	a_2	a_3
Ru−**Re3A**$^{5+}$	638	0.087	8 ± 0.1	133 ± 4.9	902 ± 1.9	55	11	34	*e*	39	61	*e*	9	91
Ru−**Re3B**$^{5+}$	638	0.093	11 ± 0.1	108 ± 0.4	856 ± 0.7	90	9	1	*e*	66	34	*e*	*e*	100
Ru−**Re5**$^{7+}$	638	0.090	11 ± 0.1	71 ± 2.2	861 ± 1.1	91	7	1	*e*	55	27	*e*	0	96
				150 ± 10.1			1			18			4	
Re2^{2+}	515	0.084	537 ± 2.0			100			100					
Re3^{3+}	570	0.156	15 ± 0.2	893 ± 2.2		96	4		*e*	100				
Re5^{5+}	570	0.113	16 ± 0.3	803 ± 1.3		93	7		*e*	100				

[a] Measured in a degassed MeCN solution at 25 °C. The excitation wavelength was 350 nm. [b] Emission maximum. [c] Quantum yield of emission. [d] Percentages of pre-exponential factors, that is, $a_n = A_n/\sum_{m=1}^{3} A_m$ (see eq 2). [e] A rise of emission was observed at the first stage. See Figure 3c.

tion of the pre-exponential factors of each component was shaded by changes in the detection wavelength. By monitoring at 470 nm, which is close to the emission maximum of the terminal Re(I) units,[40,41] the decay component with a lifetime of 8 ± 0.1 ns was dominant (Figure 3a). This component increased with the detected wavelength to 570 and 620 nm, which are the emission maxima of the interior Re(I) unit and the Ru(II) unit, respectively (see the inset in Figure 3c). The pre-exponential factors with lifetimes of 133 ± 4.9 and 902 ± 1.9 ns were similar to each other during monitoring at 570 nm, and the 902 ns component was dominant at 620 nm. Using 480 nm excitation light, which can be absorbed only by the Ru(II) unit, the emission decay curves could be fitted with a single-exponential function with a lifetime of 902 ± 1.9 ns. These results indicate that the three components with lifetimes of 8, 133, and 902 ns are a result of the emission from the terminal Re(I) units, the interior Re(I) unit, and the Ru(II) unit, respectively.

Table 2 summarizes the emission properties of the Ru(II)−Re(I) multinuclear complexes and the corresponding model complexes, that is, **Ru**$^{2+}$ for the Ru(II) unit, **Re2**$^{2+}$ for the terminal Re(I) unit, and **Re3**$^{3+}$ and **Re5**$^{5+}$ for the Re chain. A comparison of the lifetimes of **Ru**−**Re3A**$^{5+}$ with those of the model complexes indicates that the intramolecular energy transfer proceeded both from the excited interior Re(I) unit to the Ru(II) unit and also from the excited terminal Re(I) unit to both the interior Re(I) unit and the Ru(II) unit (Scheme 3a). The lifetime of the terminal Re(I) unit in **Ru**−**Re3A**$^{5+}$ (τ_1 = 8 ± 0.1 ns) was shorter than that of **Re3**$^{3+}$ (15 ± 0.2 ns), because of the additional energy transfer pathway to the Ru(II) unit (Scheme 3a). The energy transfer in **Re3**$^{3+}$ occurs from the terminal Re(I) unit only to the interior Re(I) unit (Scheme 3e). The energy transfer rate constant from the excited terminal Re(I) unit to the interior Re(I) unit (k_1(Re3^{3+}) in Scheme 3e) and the summed rate constant of the radiative and nonradiative decays from each Re(I) units in **Re3**$^{3+}$ can be determined as k_1(Re3^{3+}) = 6.5 × 10^7 s^{-1}, k_r(Re3^{3+}, terminal) + k_{nr}(Re3^{3+}, terminal) = 1.9 × 10^6 s^{-1}, and k_r(Re3^{3+}, interior) + k_{nr}(Re3^{3+}, interior) = 1.1 × 10^6 s^{-1} using the same procedures that were reported previously[33] (Supporting Information). These data are used as the energy transfer rate constant k_1(Ru−Re3A^{5+}) in Scheme 3a, and radiative and nonradiative decay rate constants form each Re(I) unit in **Ru**−**Re3A**$^{5+}$ (k_r(Ru−Re3A^{5+}, terminal) + k_{nr}(Ru−Re3A^{5+}, terminal)) because there is no strong electrical interaction between the Ru(II) unit and the Re chain in **Ru**−**Re3A**$^{5+}$. Therefore, the direct energy transfer rate from the terminal Re(I) unit to the Ru(II) unit (k_3(Ru−Re3A^{5+})) can be estimated with the following equation:

(40) Koike, K.; Hori, H.; Ishizuka, M.; Westwell, J. R.; Takeuchi, K.; Ibusuki, T.; Enjouji, K.; Konno, H.; Sakamoto, K.; Ishitani, O. *Organometallics* **1997**, *16*, 5724–5729.
(41) Tsubaki, H.; Tohyama, S.; Koike, K.; Saitoh, H.; Ishitani, O. *Dalton Trans.* **2005**, 385–395.

Scheme 3. Energy Transfer Processes and Their Rate Constants in the Ru(II)−Re(I) Multinuclear and the Corresponding Model Complexes[a]

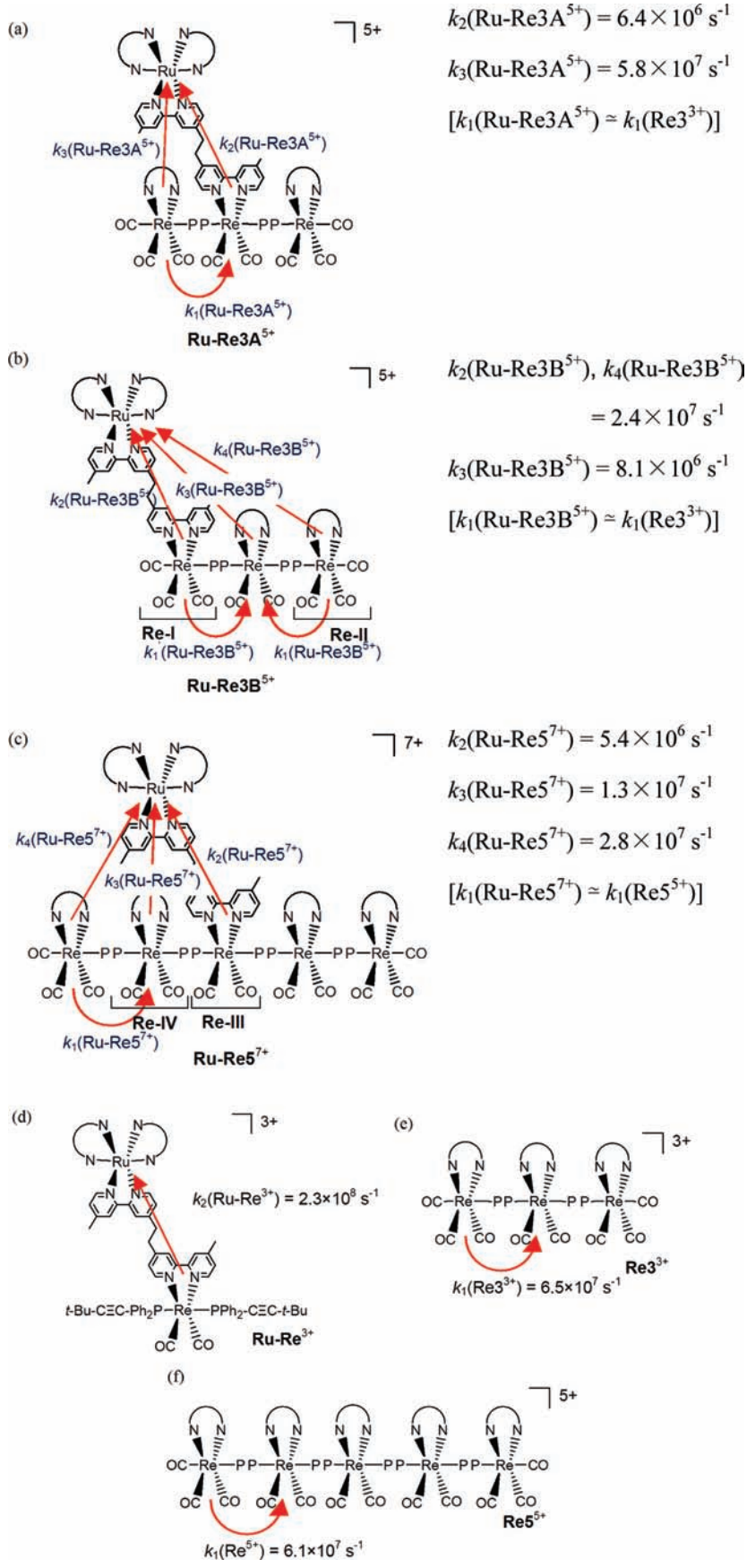

[a] Assumptions for the calculation are written in brackets.

$$k_3(\mathrm{Ru-Re3A^{5+}}) \cong \frac{1}{\tau_1(\mathrm{Ru-Re3A^{5+}})} - [k_r(\mathrm{Re3^{3+}}, \text{terminal}) + k_{nr}(\mathrm{Re3^{3+}}, \text{terminal})] - k_1(\mathrm{Re3^{3+}}) = 5.8 \times 10^7\ \mathrm{s^{-1}} \quad (3)$$

Although energy transfer from the terminal Re(I) unit to the interior Re(I) unit affected the emission profile of the excited state of the interior Re(I) unit, its decay curve can be easily separated from the rise caused by the energy transfer because the time scales were very different. Eenergy transfer should not proceed from the excited interior Re(I) unit to the terminal Re(I) unit because the energy transfer is endothermic ($\Delta E = 0.23$ eV). Therefore, the following method can be applied to calculate the rate constant of the energy transfer from the interior Re(I) unit to the Ru(II) unit (k_2(Ru−Re3A^{5+}) in Scheme 3a):

$$k_2(\mathrm{Ru-Re3A^{5+}}) = \frac{1}{\tau_2(\mathrm{Ru-Re3A^{5+}})} - [k_r(\mathrm{Ru-Re3A^{5+}}, \text{interior}) + k_{nr}(\mathrm{Ru-Re3A^{5+}}, \text{interior})] \cong \frac{1}{\tau_2(\mathrm{Ru-Re3A^{5+}})} - [k_r(\mathrm{Re3^{3+}}, \text{interior}) + k_{nr}(\mathrm{Re3^{3+}}, \text{interior})] = 6.4 \times 10^6\ \mathrm{s^{-1}} \quad (4)$$

Using these energy transfer rates, we can estimate the fates of the excited states of the Re(I) units produced in **Ru**−**Re3A**$^{5+}$ (Scheme 4). We have reported that linear-shaped Re(I) oligomers such as **Re3**$^{3+}$ have no strong interaction between the Re(I) units. Therefore, the ratio of the absorbed photons between the two terminal Re(I) units and the interior Re(I) unit was 7:3 at 350 nm using the data for **Re2**$^{2+}$. Because the spectrum of **Ru**−**Re3A**$^{5+}$ was very similar to the 1:1 summation of the spectra of **Ru**$^{2+}$ and **Re3**$^{3+}$ (Figure 1), the ratio of the absorbed photons between the terminal and the interior Re(I) unit in the Re chain of **Ru**−**Re3A**$^{5+}$ is also approximately 7:3. When 100 photons are absorbed by the Re chains of **Ru**−**Re3A**$^{5+}$, 70 of those photons are absorbed by the terminal Re(I) units. The ratio of the energy transfer rates from the terminal Re(I) unit to the interior Re(I) unit and to the Ru(II) unit, that is, k_1(Ru−Re3A^{5+}): k_3(Ru−Re3A^{5+}), was 6.5:5.8 (Scheme 3a). Because 99% of the excited terminal Re(I) units was quenched by the energy transfer (see the Supporting Information), energy transfer from the produced excited state makes both 36.5 of the excited interior Re(I) units and 32.5 of the excited Ru(II) units. Although 15% of the excited states of the internal Re(I) units, that is, $(30 + 36.5) \times 0.15 \simeq 10$, are deactivated via radiative and nonradiative decays, energy transfer also occurs to make 56.5 of the excited Ru(II) units (Supporting Information). Therefore, 89 of the excited Ru(II) units are finally produced. The energy transfer efficiency from the Re chain to the Ru(II) unit calculated by this manner (89%) is consistent with the energy transfer efficiency that was estimated from the emission spectra using eq 1 as described above (86%).

We synthesized [Ru(dmb)$_2$(C2dmb)Re(CO)$_2${PPh$_2$(C≡C−*t*-Bu)}$_2$]$^{3+}$ (**Ru**−**Re**$^{3+}$ in Scheme 3d) as a model of the central Ru(II)−Re(I) part in **Ru**−**Re3A**$^{5+}$ and determined that the energy transfer rate from the excited Re(I) unit to the Ru(II) unit in the model was k_2(Ru−Re^{3+}) $= 2.3 \times 10^8$ s^{-1}, which is much faster than k_2(Ru−Re3A^{5+}). This result strongly suggests that the intramolecular energy transfer from the excited Re(I) unit to the Ru(II) unit in both **Ru**−**Re**$^{3+}$ and **Ru**−**Re3A**$^{5+}$ proceeds via collision between them. The steric hindrance of the two terminal Re(I) units of **Ru**−**Re3A**$^{5+}$ should obstruct the collision, and, consequently, the energy transfer slowed down.

Scheme 4. Fates of the Excited States of the Re(I) Units Produced in **Ru**−**Re3A**$^{5+}$ [a]

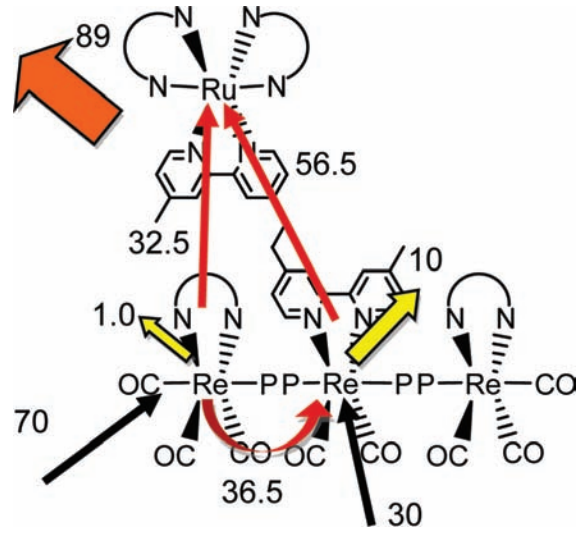

[a] The black arrows are absorbed photons processes, and the red arrows are energy transfer processes.

The emission and lifetime data of **Ru**−**Re3B**$^{5+}$, to which the Ru(II) unit is connected with one of the terminal Re(I) units, were compared to those of **Ru**−**Re3A**$^{5+}$. Because the energy transfer from the excited Re(dmb)(CO)$_2$ unit to the Re(dmb)-(CO)$_3$ unit is a highly endergonic reaction, it should be very slow. For **Ru**−**Re3B**$^{5+}$, therefore, we can obtain the direct energy transfer rate constant from the excited interior Re(I) unit, which has the Re(dmb)(CO)$_2$ structure, to the Ru(II) unit by using the decay rate constants of excited **Re3**$^{3+}$ and the following equation:

$$k_3(\mathrm{Ru-Re3B^{5+}}) \cong \frac{1}{\tau_2(\mathrm{Ru-Re3B^{5+}})} - [k_r(\mathrm{Re3^{3+}}, \text{interior}) + k_{nr}(\mathrm{Re3^{3+}}, \text{interior})] = 8.1 \times 10^6\ \mathrm{s^{-1}} \quad (5)$$

The rate constant k_2(Ru−Re3A^{5+}) is slightly but obviously slower than k_3(Ru−Re3B^{5+}), although the structures of the energy donor and the acceptor are very similar between **Ru**−**Re3B**$^{5+}$ and **Ru**−**Re3A**$^{5+}$. These results also indicate that the energy transfer from the excited Re(I) unit to the Ru(II) unit occurs via collision but the Förster-type mechanism is not dominant. In **Ru**−**Re3B**$^{3+}$, two kinds of the tricarbonyl Re(I) units [Re(LL)(CO)$_3$P−]$^+$ occur (**Re**−**I** and **Re**−**II** in Figure 3b). One of these units (**Re**−**I**) is directly connected to the Ru(II) unit. However, only one emission lifetime component was attributed to the tricarbonyl units ($\tau = 11$ ns). Consequently, the energy transfer rates from the excited **Re**−**I** and **Re**−**II** units to the Ru(II) unit (k_2(Ru−Re3B^{5+})) and k_4(Ru−Re3B^{5+}) should be similar each other.

Four kinds of emitters in **Ru**−**Re5**$^{7+}$ exist (Scheme 3c): the Ru(II) unit, two kinds of the [Re(dmb)(CO)$_2$(PP)$_2$] type units (**Re**−**III** and **Re**−**IV**), and the terminal Re(I) unit. If the energy transfer rate from the excited terminal Re(I) unit to the interior unit **Re**−**IV** (k_1(Ru−Re5^{7+})) is the same to that of **Re5**$^{5+}$ (k_1(Re5^{5+}) $= 6.1 \times 10^7$ s^{-1}), k_4(Ru−Re5^{7+}) can be estimated as 2.8×10^7 s^{-1} by the same procedures used for k_3(Ru−Re3A^{5+}). The energy migration phenomenon between

the interior units in the linear-shaped Re oligomers and polymers is not well understood.[33a] Two lifetime components of 71 and 150 ns were observed and attributable to the interior Re(I) units. Therefore, the energy migration processes between the interior Re(I) units should be much slower than energy transfers from these Re(I) units to the Ru(II) unit ($k_m \ll 3.73 \times 10^6$ s^{-1}: see the Supporting Information). We can estimate the energy transfer rates as k_3(Ru−Re5^{7+}) = 1.3×10^7 s^{-1} and k_2(Ru−Re5^{7+}) = 5.4×10^6 s^{-1} using τ = 71 and 150 ns because of the structural and environmental similarities to the interior Re(I) units in **Ru−Re3B**$^{5+}$ (k_3(Ru−Re3B^{5+}) = 8.1×10^6 s^{-1}) and **Ru−Re3A**$^{5+}$ (k_2(Ru−Re3A^{5+}) = 6.4×10^6 s^{-1}), respectively.

In Scheme 3, the energy transfer rate from each excited Re(I) unit to the Ru(II) unit or to the other Re(I) unit can be summarized. In **Ru−Re3B**$^{5+}$ and **Ru−Re5**$^{7+}$, both of the energy transfer efficiencies from the excited Re chain to the Ru(II) unit were calculated as 89% by procedures similar to those for **Ru−Re3A**$^{5+}$.

Conclusion

We have successfully synthesized linear Re(I) trinuclear and pentanuclear complexes with the Ru(II) trisdiimine complex as an energy acceptor. All of the Ru(II)−Re(I) multinuclear complexes were emissive, mostly from the Ru(II) unit, at room temperature in solution. In these complexes, photoinduced intramolecular energy transfer proceeded efficiently from the excited Re(I) units to the Ru(II) unit. All of these energy transfer rate constants and efficiencies could be estimated using the photophysical data of the corresponding model complexes.

Both the dmb ligand on the Ru(II) unit and the CO ligand on the terminal Re(I) units can be substituted with various types of ligands, and, therefore, this type of heteronuclear complex can potentially be used as a constituent unit in a new series of light-harvesting materials. We have already found that **Ru−Re3A**$^{5+}$ works as an effective photocatalyst for CO_2 reduction. The possibilities including this preliminary result are currently under investigation in our laboratory.

Experimental Section

Instrumentation and Measurements. The IR spectra were recorded in an MeCN solution with a JASCO FT/IR-610 spectrometer at 1 cm^{-1} resolution. The ^{1}H and H,H COSY NMR spectra were measured in an acetone-d_6 solution using a JEOL JNM-AL400 (400 MHz). The residual protons of the acetone-d_6 were used as internal standards for the measurements. The electrospray ionization mass spectra (ESI MS) were measured using a Shimadzu LCMS-2010A mass spectrometer or a Waters LCT Premier XE ESI TOFMS spectrometer. The UV/vis absorption spectra were recorded in an MeCN solution with a JASCO V-565 spectrophotometer. The emission spectra were recorded at 25 °C using a JASCO FP-6500 spectrophotometer, and the correction data for the detector sensitivity were supplied by JASCO. The sample solutions were degassed by the freeze−pump−thaw method before the emission measurements. The emission quantum yields were evaluated with emission from Ru(bpy)$_3^{2+}$ in degassed acetonitrile (Φ_{em} = 0.095).[42]

(42) Recently, the emission quantum yield of Ru(bpy)$_3^{2+}$ has been reevaluated from Φ_{em} = 0.062 to Φ_{em} = 0.095: Suzuki, K.; Kobayashi, A.; Kaneko, S.; Takehira, K.; Yoshihara, T.; Ishida, H.; Shiina, Y.; Oishi, S.; Tobita, S. *Phys. Chem. Chem. Phys.* **2009**, *11*, 9850–9860. Although we used the new value (Φ_{em} = 0.095) as the reference in this Article, the older data (Φ_{em} = 0.062) were used in our previous paper[23] about the photophysics of the linear Re(I) oligomers and polymers. The readers should be careful about this point if they compare emission quantum yields reported in the two papers.

Photochemical Reactions. For the photochemical ligand substitution reaction, the solution was irradiated by an Eikosha 500 W high-pressure mercury lamp with a uranium glass filter (>330 nm) in a Pyrex doughnut-form cell. N_2 gas was bubbled through the solution at 50−60 °C.

Separation Using Size Exclusion Chromatography. Separation of the multinuclear complexes was achieved by size exclusion chromatography (SEC) using a pair of Shodex PROTEIN KW-2002.5 columns (300 mm × 20.0 mm i.d.) with a KW-LG guard-column (50 mm × 8.0 mm i.d.) and a JAI LC-9201 recycling preparative HPLC apparatus with a JASCO 870-UV detector. The eluent was a 1:1 (v/v) mixture of methanol and acetonitrile with 0.15 M $CH_3CO_2NH_4$, and the flow rate was 5.0 mL min^{-1}. Details have been reported elsewhere.[37]

Emission Lifetime Measurement. An acetonitrile solution of the metal complex was degassed by the freeze−pump−thaw method and then transferred into a 10 × 10 × 40 mm quartz cuvette. The emission lifetimes were measured using a Horiba NAES-1100 or FluoroCube 3000U time-correlated single-photon-counting system. The sample solutions were excited by an NFL-111 ns H_2 lamp with a proper band-pass filter (Toshiba U350) for the NAES-1100 or by a Nano LED-370 (371 nm) for the FluoroCube. The decay profile simulations were performed by a nonlinear least-squares method.

Materials. The THF was distilled from Na/benzophenone just before use. The acetonitrile was dried three times over P_2O_5 and then distilled from CaH_2 prior to use. Dichloromethane was dried over CaH_2 prior to use. All purified solvents were kept under N_2 before use. Spectral-grade solvents were used for the spectroscopic measurements. Other reagents and solvents were purchased reagent-grade and used without further purification.

Synthesis. The standard Schlenk techniques were employed for synthesis. Ru(dmb)$_2$(C2dmb)Re(CO)$_3$Cl (**Ru−Re(CO)$_3$Cl**$^{2+}$), *fac*-Re(CO)$_3$(dmb)(CF$_3$SO$_3$), [Re(dmb)(CO)$_3$−**PP**−Re(dmb)(CO)$_2$(CF$_3$SO$_3$)]$^+$, and the corresponding model complexes were prepared according to the method in the literature.[33,34]

[Ru(dmb)$_2$(C2dmb)Re(CO)$_2${−PP−Re(dmb)(CO)$_2$−PP−Re(dmb)(CO)$_3$}$_2$](PF$_6$)$_7$, (Ru−Re5^{7+})(PF$_6^-$)$_7$. The synthesis procedure for **Ru−Re5**$^{7+}$ is summarized in Scheme 5. A dichloromethane solution (100 mL) of **Ru−Re(CO)$_3$Cl**$^{2+}$(PF$_6^-$)$_2$ (100 mg, 0.07 mmol) with 1 equiv of Tl(CF$_3$SO$_3$) (25 mg, 0.07 mmol) was refluxed for 1 day in dim light, giving [Ru(dmb)$_2$(C2dmb)Re(CO)$_3$(CF$_3$SO$_3$)]$^{2+}$(PF$_6^-$)$_2$ (**Ru−Re(CO)$_3$(CF$_3$SO$_3$)**$^{2+}$). A dichloromethane solution (100 mL) of **Ru−Re(CO)$_3$(CF$_3$SO$_3$)**$^{2+}$ (90 mg, 0.06 mmol) with bis(diphenylphosphino)acetylene (**PP**) (118 mg, 0.30 mmol) was stirred at room temperature in dim light for 1 day, giving [Ru(dmb)$_2$(C2dmb)Re(CO)$_3$(η^1-**PP**)]$^{3+}$ (**Ru−Re(CO)$_3$(η^1-PP)**$^{3+}$). Next, 100 mL of THF was added, and the solution was irradiated at 50 °C for 8 h using a high-pressure mercury lamp with a uranium glass filter (>330 nm). The result was [Ru(dmb)$_2$(C2dmb)Re(CO)$_2$(η^1-**PP**)$_2$]$^{3+}$ (**Ru−Re(CO)$_2$(η^1-PP)$_2$**$^{3+}$). The solvent was evaporated, and the residual red solid was washed several times with degassed ether. A dichloromethane solution (100 mL) containing **Ru−Re(CO)$_2$(η^1-PP)$_2$**$^{3+}$ and 2 equiv of [Re(dmb)(CO)$_3$−**PP**−Re(dmb)(CO)$_2$(CF$_3$SO$_3$)]$^+$ was stirred at room temperature for 1 day and then at 50 °C for 1 day in dim light. After the solution was evaporated, the residue was separated using SEC. The band, which included the product, was evaporated under reduced pressure and dissolved in a small amount of methanol. The solution was added dropwise to a concentrated MeOH solution of NH_4PF_6. The precipitated orange powder was filtered off, washed with diethylether, and then dried in a vacuum. Yield: 13%. Anal. Calcd for $C_{212}H_{172}F_{42}N_{16}O_{12}P_{15}Re_5Ru_1$: C, 46.89; H, 3.19; N, 4.13. Found: C, 46.82; H, 3.41; N, 4.22. ^{1}H NMR (δ, 400 MHz, CD_3COCD_3): 8.73 (s, 1H, α-3), 8.67 (s, 1H, β-3), 8.65 (s, 4H, dmb-3,3′ of Ru(dmb)$_2$), 8.52, 8.48 (d, 4H, J = 7.6 Hz, dmb-6,6′ of terminal-Re(dmb)(CO)$_3$), 8.20, 8.11 (s, 4H, dmb-3,3′ of terminal-Re(dmb)(CO)$_3$), 7.94 (d, 1H, J = 5.4 Hz, α-6), 7.90 (s, 1H, γ-3), 7.84 (s, 1H, δ-3), 7.83 (d, 4H, J = 5.6 Hz, dmb-6,6′ of Ru(dmb)$_2$), 7.81 (d, 1H, J = 5.4 Hz, β-6), 7.80 (d, 1H, J = 5.1 Hz, δ-6), 7.77

Scheme 5. Synthesis of **Ru**−**Re5**$^{7+}$ [a]

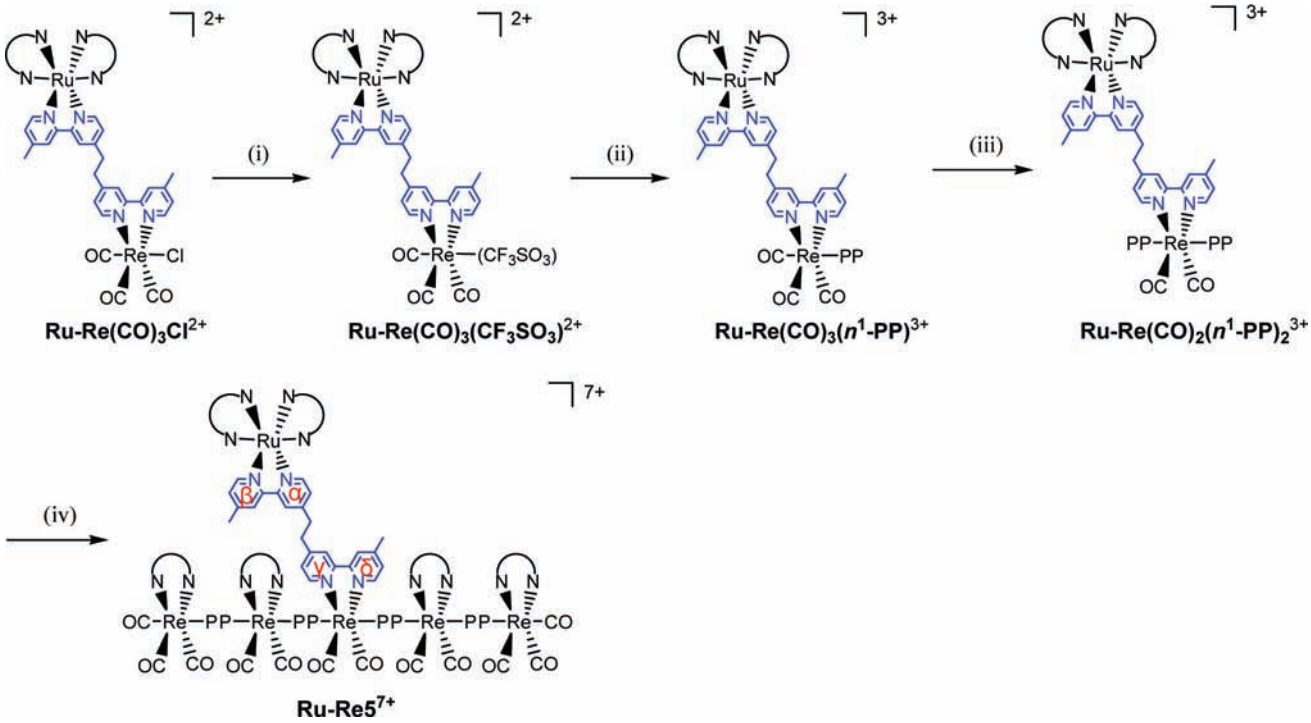

[a] Reagents and reaction conditions: (i) $Tl(CF_3SO_3)$ (1 equiv) in CH_2Cl_2 reflux for 2 days; (ii) excess **PP** in CH_2Cl_2 at room temperature for 1 day and then at 40 °C for 1 day; (iii) $h\nu$ (>330 nm) in CH_2Cl_2 at 50 °C for 8 h; and (iv) $[Re(dmb)(CO)_3-\mathbf{PP}-Re(dmb)(CO)_2(CF_3SO_3)]^+$ (2 equiv) in CH_2Cl_2 at room temperature for 1 day and then at 40 °C for 1 day.

Scheme 6. Synthesis of **Ru**−**Re3A**$^{5+}$ [a]

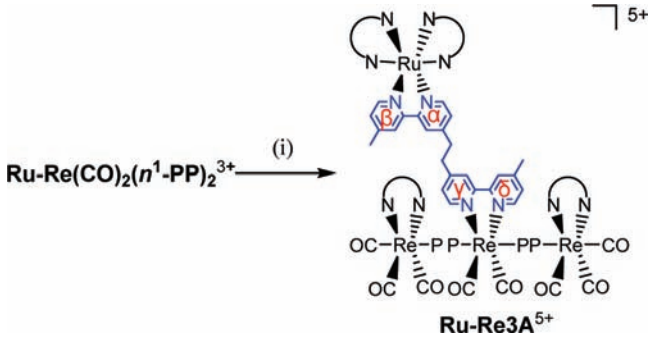

[a] Reagents and reaction conditions: (i) $[Re(dmb)(CO)_3-\mathbf{PP}-Re(dmb)(CO)_2(CF_3SO_3)]^+$ (2 equiv) in CH_2Cl_2 at room temperature for 1 day and then at 40 °C for 1 day.

Scheme 7. Synthesis of **Ru**−**Re3B**$^{5+}$ [a]

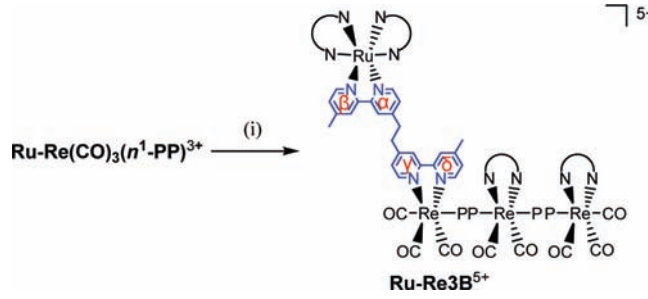

[a] All complexes were PF_6 salts. Reagents and reaction conditions: (i) 1 equiv of $[Re(dmb)(CO)_3-\mathbf{PP}-Re(dmb)(CO)_2(CF_3SO_3)]^+$ in CH_2Cl_2 at room temperature for 1 day and then at 40 °C for 1 day.

(d, 1H, J = 5.1 Hz, γ-6), 7.70, 7.61 (s, 4H, dmb-6 of **Re**−**IV**), 7.65−7.24 (m, 84H, α,β,δ,γ-5, and Ph), 7.58, 7.57 (d, 4H, J = 5.6 Hz, dmb-6 in **Re**−**IV**), 7.37 (d, 4H, J = 5.6 Hz, dmb-5 in $Ru(dmb)_2$), 6.92, 6.88 (d, 4H, J = 7.6 Hz, dmb-5 of terminal-$Re(dmb)(CO)_3$), 6.48, 6.39 (d, 4H, J = 5.6 Hz, dmb-5 of **Re**−**IV**). IR (MeCN): ν_{CO}/cm^{-1} = 2044 (s), 1961 (s), 1929 (m), 1884 (m). ESI MS in MeCN (m/z): 630.8 $[M]^{7+}$, 760.1 $[M + PF_6]^{6+}$, 941.1 $[M + 2PF_6]^{5+}$.

$[Ru(dmb)_2(C2dmb)Re(CO)_2\{-PP-Re(dmb)(CO)_3\}_2](PF_6)_5$, $(Ru-Re3A^{5+})(PF_6^-)_5$. A similar procedure for **Ru**−**Re$_5$**$^{7+}$ was applied to the synthesis of **Ru**−**Re3A**$^{5+}$ using *fac*-$Re(dmb)(CO)_3(CF_3SO_3)$ instead of $[Re(dmb)(CO)_3-\mathbf{PP}-Re(dmb)(CO)_2(CF_3SO_3)]^+$ (Scheme 6). Yield: 16%. Anal. Calcd for $C_{132}H_{110}F_{30}N_{12}O_8P_9Re_3Ru$: C, 45.29; H, 3.17; N, 4.80. Found: C, 45.21; H, 3.39; N, 4.55. ^{1}H NMR (δ, 400 MHz, CD_3COCD_3): 8.82 (s, 1H, α-3), 8.67 (s, 1H, β-3), 8.65 (s, 4H, dmb-3,3′ of $Ru(dmb)_2$), 8.53, 8.47 (d, 4H, J = 5.4 Hz, dmb-6,6′ of terminal-$Re(dmb)(CO)_3$), 8.14, 8.10 (s, 4H, dmb-3,3′ of terminal-$Re(dmb)(CO)_3$), 7.94 (d, 1H, J = 5.4 Hz, α-6), 7.90 (s, 1H, γ-3), 7.84 (s, 1H, δ-3), 7.83 (d, 4H, J = 5.6 Hz, dmb-6,6′ of $Ru(dmb)_2$), 7.81 (d, 1H, J = 5.4 Hz, β-6), 7.80 (d, J = 5.1 Hz, 1H, δ-6), 7.77 (d, J = 5.1 Hz, 1H, γ-6), 7.65−7.24 (m, 44H, α, β, δ, γ-5, and Ph), 7.37 (d, 4H, J = 5.6 Hz, dmb-5 of $Ru(dmb)_2$), 7.18, 7.15 (d, 4H, J = 5.4 Hz, dmb-5 of terminal-$Re(dmb)(CO)_3$). IR (MeCN): ν_{CO}/cm^{-1} = 2044 (s), 1960 (b), 1929 (m), 1884 (s). ESI MS in MeCN (m/z): 555.2 $[M]^{5+}$, 730.2 $[M + PF_6]^{4+}$.

$[Ru(dmb)_2(C2dmb)Re(CO)_3-PP-Re(dmb)(CO)_2-PP-Re(dmb)(CO)_3](PF_6)_5$, $(Ru-Re3B^{5+})(PF_6^-)_5$. The synthesis procedure for **Ru**−**Re3B**$^{5+}$ is shown in Scheme 7. A dichloromethane solution (100 mL) containing **Ru**−**Re(CO)$_3$(η^1-PP)**$^{3+}$ (100 mg, 0.05 mmol) and an equivalent of $[Re(dmb)(CO)_3-\mathbf{PP}-Re(dmb)(CO)_2(CF_3SO_3)]^+$ (81 mg, 0.05 mmol) was stirred at room temperature in dim light for 1 day. The resulting **Ru**−**Re3B**$^{5+}$ was isolated using a method similar to the one used to isolate **Ru**−**Re5**$^{7+}(PF_6^-)_7$. Yield: 21%. Anal. Calcd for $C_{132}H_{110}F_{30}N_{12}O_8P_9Re_3Ru$: C, 45.29; H, 3.17; N, 4.80. Found: C, 45.19; H, 3.47; N, 4.64. ^{1}H NMR (δ, 400 MHz, CD_3COCD_3): 8.82 (s, 1H, α-3), 8.70 (s, 1H, γ-3), 8.67 (s, 1H, β-3), 8.65 (s, 4H, dmb-3,3′ of $Ru(dmb)_2$), 8.61 (d, 1H, J = 5.4 Hz, γ-6), 8.52, 8.48 (d, 4H, J =

Scheme 8. Synthesis of **Ru**−**Re**$^{3+}$ [a]

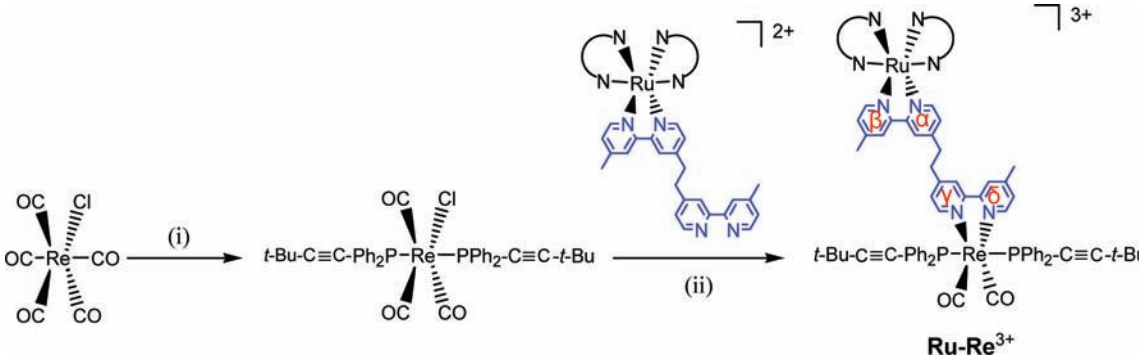

[a] Reagents and reaction conditions: (i) PPh_2−C≡C−*t*-Bu (2 equiv) in toluene reflux for 1 day; (ii) $Ag(CF_3SO_3)$ (1 equiv) in THF reflux for 3 h; and (iii) in acetone/*o*-dichlorobenzene (1:3 v/v) reflux for 1 day.

7.6 Hz, dmb-6,6′ of $Re(dmb)(CO)_3$), 8.20, 8.11 (s, 4H, dmb-3,3′ of **Re**−**II**), 7.94 (d, 1H, J = 5.4 Hz, α-6), 7.83 (d, 4H, J = 5.6 Hz, dmb-6,6′ of $Ru(dmb)_2$), 7.79 (s, 1H, δ-3), 7.81 (d, 1H, J = 5.4 Hz, β-6), 7.70 (s, 2H, dmb-3,3′ of interior $Re(dmb)(CO)_2$), 7.60−7.27 (m, 49H, α, β, δ, γ-5, δ-6, and dmb-5,5′ in $Ru(dmb)_2$), 7.58, 7.57 (d, 2H, J = 7.08 Hz, dmb-6,6′ of interior $Re(dmb)(CO)_2$), 7.08, 6.62 (d, 2H, J = 7.08 Hz, dmb-5,5′ of interior $Re(dmb)(CO)_2$), 6.92, 6.88 (d, 2H, J = 7.56 Hz, dmb-5,5′ of **Re**−**II**). IR (MeCN): ν_{CO}/cm^{-1} = 2044 (s), 1960 (b), 1929 (m), 1884 (s). ESI MS in MeCN (*m*/*z*): 555.2 $[M]^{5+}$, 730.2 $[M + PF_6]^{4+}$, 1022.0 $[M + 2PF_6]^{3+}$.

Synthesis and Identification of the Model Complexes. Similar synthesis procedures for the corresponding 2,2′-bipyridine complexes[33] were applied for the synthesis of the linear-type of Re(I) oligomers with 4,4′-dimethyl-2,2′-bipyridine (dmb), that is, $[Re(dmb)(CO)_3$−**PP**−$Re(dmb)(CO)_3]^{2+}$ (**Re2**$^{2+}$), $[Re(dmb)(CO)_3$−**PP**−$Re(dmb)(CO)_2$−**PP**−$Re(dmb)(CO)_3]^{3+}$ (**Re3**$^{3+}$), and $[Re(dmb)(CO)_3\{$−**PP**−$Re(dmb)(CO)_2\}_3$−**PP**−$Re(dmb)(CO)_3]^{5+}$ (**Re5**$^{5+}$).

Re2^{2+}, yield: 90%. ^{1}H NMR (δ, 400 MHz, CD_3COCD_3): 8.54 (d, 4H, J = 5.6 Hz, dmb-6,6′), 8.24 (s, 4H, dmb-3,3′), 7.68 (dd, 4H, J = 7.2, 6.8 Hz, Ph-*p*), 7.53 (m, 8H, J = 7.2, 6.8, 2.4 Hz, Ph-*m*), 7.26 (d, 8H, J = 6.8, Ph-*o*), 7.24 (d, 4H, J = 5.6 Hz, dmb-5,5′). IR (CH_2Cl_2): ν_{CO}/cm^{-1} = 2045, 1962, 1930. ESI-MS in MeCN (*m*/*z*): 652 $[M]^{2+}$.

Re3^{3+}, yield: 64%. Anal. Calcd for $C_{96}H_{74}F_{18}N_6O_8P_7Re_3Ru$: C, 45.09; H, 2.92; N, 3.29. Found: C, 45.20; H, 3.01; N, 3.22. ^{1}H NMR (δ, 400 MHz, CD_3COCD_3): 8.52 (d, 4H, J = 5.8 Hz, dmb-6,6′ of $Re(dmb)(CO)_3$), 8.11 (s, 4H, dmb-3,3′ of $Re(dmb)(CO)_3$), 7.75 (d, 2H, J = 6.1 Hz, dmb-6,6′ of $Re(dmb)(CO)_2$), 7.73 (s, 2H, dmb-3,3′ of $Re(dmb)(CO)_2$), 7.64−7.58 (dd, 8H, J = 7.2, 6.8 Hz, Ph-*p*), 7.49−7.41 (m, 16H, Ph-*m*), 7.26 (d, 8H, J = 6.8 Hz,Ph-*o*), 7.24 (d, 4H, J = 5.6 Hz, dmb-5,5′ of $Re(dmb)(CO)_3$), 7.11 (dd, 8H, J = 7.2, 6.8 Hz, Ph-*o*), 6.58 (d, 2H, J = 5.2 Hz, dmb-5,5′ of $Re(dmb)(CO)_2$). IR (CH_2Cl_2): ν_{CO}/cm^{-1} = 2044, 1960, 1929, 1884. ESI-MS in MeCN (*m*/*z*): 708.2 $[M]^{3+}$, 1133.6 $[M + PF_6]^{2+}$.

Re5^{5+}, yield: 52%. Anal. Calcd for $C_{176}H_{138}F_{35}N_{10}O_{12}P_8Re_5$: C, 47.73; H, 3.14; N, 3.16. Found: C, 47.89; H, 3.22; N, 3.41. ^{1}H NMR (δ, 400 MHz, CD_3COCD_3): 8.50 (d, 4H, J = 6.1 Hz, dmb-6,6′ of $Re(dmb)(CO)_3$), 8.10 (s, 4H, dmb-3,3′ of $Re(dmb)(CO)_3$), 7.74 (d, 4H, J = 6.1 Hz, dmb-6,6′ of $Re(dmb)(CO)_2$), 7.72 (s, 4H, dmb-3,3′ of $Re(dmb)(CO)_2$), 7.64−7.58 (dd, 8H,, J = 7.2, 6.8 Hz, Ph-*p*), 7.49−7.41 (m, 16H, Ph-*m*), 7.26 (d, 8H, J = 6.8 Hz,Ph-*o*), 7.24 (d, 8H, J = 5.6 Hz, dmb-5,5′ of $Re(dmb)(CO)_3$), 7.11 (dd, 8H, J = 7.2, 6.8 Hz, Ph-*o*), 6.49 (d, 4H, J = 6.1 Hz, dmb-5,5′ of $Re(dmb)(CO)_2$), 6.46 (d, 2H, J = 6.1 Hz, dmb-5,5′ in $Re(dmb)(CO)_2$). IR (CH_2Cl_2): ν_{CO}/cm^{-1} = 2044, 1960, 1955, 1929, 1883. ESI-MS in MeCN (*m*/*z*): 753.3 $[M]^{5+}$, 977.2 $[M + PF_6]^{4+}$.

$[Ru(dmb)_2(C2dmb)Re(CO)_2\{PPh_2(C\equiv C-t\text{-}Bu)\}_2]^{3+}(PF_6^-)_3$, (Ru−Re^{3+})$(PF_6^-)_3$. The synthesis procedure for **Ru**−**Re**$^{3+}$ is shown in Scheme 8. A toluene solution (100 mL) of $Re(CO)_5Cl$ (100 mg, 0.28 mmol) with 2 equiv of PPh_2−C≡C−*t*-Bu was refluxed in dim light for 1 day, giving $Re(CO)_3(PPh_2$−C≡C−*t*-$Bu)_2Cl$. The solvent was evaporated under reduced pressure, and 50 mL of THF was added to the residue. The THF solution of $Re(CO)_3(PPh_2$−C≡C−*t*-$Bu)_2Cl$ with an equivalent of $Ag(CF_3SO_3)$ was refluxed in dim light for 3 h, giving $Re(CO)_3(PPh_2$−C≡C−*t*-$Bu)_2(CF_3SO_3)$. The solvent was evaporated under reduced pressure, and 30 mL of acetone was added to the residue. A mixed solution of acetone and *o*-dichlorobenzene (1:3 v/v) of $Re(CO)_3(PPh_2$−C≡C−*t*-$Bu)_2(CF_3SO_3)$ with an equivalent of $[Ru(dmb)_2(C2dmb)](PF_6)_2$ was refluxed in dim light for 1 day. The solution was evaporated, and the residue was separated using SEC. The band that included the product was evaporated under reduced pressure, and a methanol solution of the residue was added dropwise to a concentrated MeOH solution of NH_4PF_6. The precipitated yellow powders were filtered off, washed with diethylether, and then dried in a vacuum. The yield based on $[Ru(dmb)_2(C2dmb)](PF_6)_2$ used: 34%. Anal. Calcd for $C_{86}H_{84}F_{18}N_8O_2P_5ReRu$: C, 50.49; H, 4.14; N, 5.48. Found: C, 50.26; H, 4.00; N, 5.27. ^{1}H NMR (δ, 400 MHz, CD_3COCD_3): 8.82 (s, 1H, α-3), 8.66−8.69 (m, 5H, β-3 and dmb-3,3′), 8.35 (s, 1H, γ or δ-3), 8.32 (d, J = 5.7 Hz, 1H, γ or δ-6), 8.29 (s, 1H, γ or δ-3), 8.12 (d, J = 5.7 Hz, 1H, γ or δ-6), 7.94 (d, J = 5.7 Hz, 1H, α-6), 7.80−7.84 (m, 5H, β-6, dmb-6,6′ of $Ru(dmb)_2$), 7.27−7.60 (m, 28H, α, β, γ, and δ-5, dmb-5,5′ of $Ru(dmb)_2$, and Ph), 3.15−3.28 (m, 4H, $-CH_2CH_2-$), 2.52−2.58 (m, 18H, α-dmb-CH_3, δ-dmb-CH_3, dmb-CH_3 of $Ru(dmb)_2$), 1.14−1.15 (m, 18H, *t*-Bu). ESI-MS in MeCN (*m*/*z*): 537 $[M]^{3+}$, 879 $[M + PF_6]^{2+}$. FT-IR (in CH_2Cl_2) ν_{CO} (cm^{-1}): 1943, 1873.

$[Re(dmb)(CO)_2\{PPh_2(C\equiv C-t\text{-}Bu)\}_2](PF_6)$. A procedure similar to the one used for $[Re(dmb)(CO)_2\{PPh_2(C\equiv C-t\text{-}Bu)\}_2]^+$ was used to synthesize **Ru**−**Re**$^{3+}$. The reactant dmb was used instead of $[Ru(dmb)_2(C2dmb)](PF_6)_2$. Anal. Calcd for $C_{50}H_{50}F_6N_2O_2P_3Re_1$: C, 54.39; H, 4.56; N, 2.54. Found: C, 54.63; H, 4.77; N, 2.50. ^{1}H NMR (δ, 400 MHz, CD_3COCD_3): 8.31 (s, 2H, dmb-3,3′), 8.18 (d, J = 5.8 Hz, 2H, dmb-6,6′), 7.32−7.49 (m, 20H, Ph), 7.28 (d, J = 5.8 Hz, 2H, dmb-5,5′), 2.56 (s, 6H, dmb-CH_3), 1.14 (s, 18H, $-C(CH_3)_3$). IR (CH_2Cl_2): ν_{CO}/cm^{-1} = 1945, 1874. ESI MS in MeCN (*m*/*z*): 960 $[M]^+$.

Supporting Information Available: The ESI-MS and ESI-TOFMS spectra of **Ru**−**Re5**$^{7+}$ (Figures S1 and S2), the ESI-MS spectra of **Ru**−**Re3A**$^{5+}$ (Figure S3), the UV/vis absorption spectra of **Ru**−**Re3B**$^{5+}$ and the corresponding model complexes (Figure S4), the emission spectra of **Ru**−**Re5**$^{7+}$, **Ru**−**Re3B**$^{5+}$, and the corresponding model complexes (Figure S5), and the estimation methods for the energy transfer rate constant in **Re3**$^{3+}$ and the energy transfer efficiency in **Ru**−**Re3A**$^{5+}$. This material is available free of charge via the Internet at http://pubs.acs.org.

JA104601B